

# A Novel Fault Diagnosis Method for Rolling Bearings Based on ELTSA and CGWO-WGKELM

Zihang GAO\*, Wang QIU\*\*

\*Institute of Digital and Intelligent Technology, Wenzhou Vocational College of Science and Technology, Wenzhou 325006, China, E-mail: gaozihang@wzvcst.edu.cn (Corresponding Author)

\*\*School of Information and Computer Engineering, Pingxiang University, Pingxiang 337055, China

<https://doi.org/10.5755/j02.mech.42637>

## 1. Introduction

Rolling bearings serve as critical components in mechanical systems, particularly in underwater operational environments [1-5]. The intricate nature of vibration signals generated by rolling bearings presents substantial difficulties in developing reliable fault diagnosis approaches [6, 7]. The high-dimensional characteristics of rolling bearing monitoring data can adversely impact both diagnostic precision and computational efficiency [8], thereby necessitating dimensionality reduction of these features.

Due to the inherent sparsity present in many rolling bearing datasets, conventional dimensionality reduction techniques demonstrate limited effectiveness when processing such information. To overcome these limitations, this paper introduces an enhanced entropy-weighted local tangent space alignment (ELTSA) method specifically designed for dimensionality reduction of rolling bearing data. The proposed ELTSA methodology effectively resolves two fundamental challenges: inaccurate distance measurement associated with conventional Euclidean metrics and insufficient preservation of critical data information during the dimensionality reduction process.

Therefore, this article proposes a novel local tangent space alignment based on entropy-weighted distance (ELTSA) to reduce the feature dimensionality of rolling bearings data. The ELTSA algorithm can address the issue of inaccurate Euclidean distance measurement and inability to effectively preserve data information.

To enhance the fault diagnosis capability of traditional Extreme Learning Machine (ELM) for rolling bearings [9], a Weighted Gaussian Kernel ELM (WGKELM) algorithm is proposed, which replaces the hidden layer with kernel functions to significantly improve nonlinear processing capacity and robustness. However, the performance of the WGKELM algorithm is highly sensitive to its training parameters, necessitating the use of intelligent optimization methods for parameter tuning. Grey Wolf Optimization (GWO), inspired by the social hierarchy and hunting behavior of grey wolves, exhibits strong robustness [10-12]. Nevertheless, the traditional GWO algorithm suffers from limited population diversity, often leading to premature convergence and local optima trapping [13]. To address this limitation, a Circle chaotic mapping strategy is incorporated into the conventional GWO framework to enhance global exploration capabilities. This modified approach, termed Circle chaotic mapping-based GWO (CGWO), is employed to optimize the training parameters of the WGKELM algorithm.

Firstly, a novel ELTSA algorithm is presented.

Secondly, a novel WGKELM with Circle chaotic mapping-based GWO (CGWGKELM) is presented. Thirdly, experimental study is performed to testify the feasibility of the proposed fault diagnosis method for rolling bearings. Finally, conclusions are given.

## 2. The ELTSA Algorithm

It is widely recognized that LTSA employs Euclidean distance to identify the nearest neighbors during feature extraction [14, 15]. To overcome the limitations of Euclidean distance this paper introduces an entropy-weighted distance metric. This metric assigns weights to features based on their information entropy, emphasizing those with greater informational significance. Consequently, we propose an enhanced LTSA algorithm that integrates this entropy-weighted distance to improve neighborhood selection and data representation.

Given high dimensional dataset  $X = (x_1, x_2, \dots, x_L)$  ( $x_i$  is a sample with  $N$  features), calculate the information entropy  $\Omega(x_i)$

$$\Omega(x_i) = -\sum_{i=1}^N p(x_i) \log_2 p(x_i), \quad (1)$$

where  $p(x_i)$  denotes the appearing probability.

Cosine similarity of the information entropy is employed as entropy-weighted distance in this paper.

$$Dist_{cs} = \frac{\Omega(x_i) \cdot \Omega(x_j)}{\|\Omega(x_i)\| \|\Omega(x_j)\|}. \quad (2)$$

LTSA is a representative manifold learning technique capable of revealing low-dimensional structures hidden within high-dimensional observational data, enabling the recovery of essential geometric properties while preserving the critical information contained in the original dataset. Construct the neighborhood of sampling point based on the entropy-weighted distance between samples, and map the neighborhood to a local low dimensional tangent space by the local transformation matrix. Thus, approximate the nearby local structure of the sample points as follows:

$$\min \sum_{i=1}^k \|x_i H_k - R_i \lambda_i\|_F^2, \quad (3)$$

where  $\|\cdot\|_F$  denotes the Frobenius norm,  $H_k$  denotes the central matrix, and  $\lambda_i$  denotes a local low dimensional description of  $X_i$ ,

$$\lambda_i = R_i^T X_i \left( I - \frac{1}{k} e e^T \right), \quad (4)$$

where  $I$  denotes the identity matrix, and  $e$  denotes the column vector representing all elements equal to 1.

The objective function described by Eq. (3) can be transformed into the optimization problem,

$$\min \sum_{i=1}^N \|Y_i H_k - Q_i \lambda_i\|_F^2, \quad (5)$$

where  $Y_i$  denotes a  $X_i$ 's global low dimensional description, and  $Q_i$  denotes the global transformation matrix given as follows:

$$Q_i = Y_i H_k \lambda_i^*, \quad (6)$$

where  $\lambda_i^*$  denotes the  $\lambda_i$ 's Moore Penrose generalized inverse.

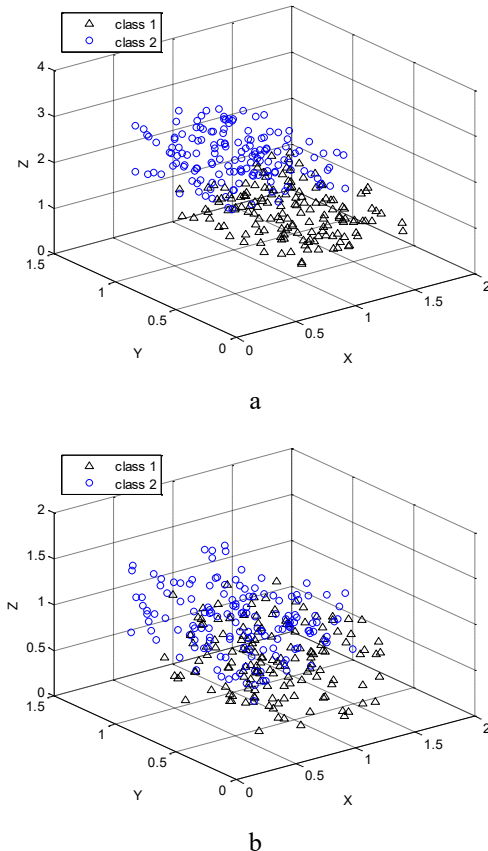


Fig. 1 Comparison of the data distribution of two classes between ELTSA and LTSA: a – the data distribution of two classes by using ELTSA, b – the data distribution of two classes by using LTSA

Finally, the corresponding low dimensional embedding datasets  $Y$  of  $X$  is shown as follows:

$$Y = \beta^T X H_k = \beta^T X \left( I - ee^T / k \right), \quad (7)$$

where  $\beta$  denotes the projection matrix.

Fig. 1 illustrates the class-wise data distributions produced by ELTSA and standard LTSA. Visibly, the overlap between the two categories is markedly smaller under ELTSA, yielding a higher class-separation rate. This confirms that incorporating the entropy-weighted distance into LTSA effectively mitigates the disturbance caused by positional misalignment of samples.

### 3. The CGWO-WGKELM Algorithm

Given the hidden layer feature mapping matrix  $M = [m(x_1), \dots, m(x_N)]^T$  and the training objective matrix  $T = [t_1, \dots, t_N]^T$ , the mathematical model of an extreme learning machine is expressed as follows:

$$\psi(x) = m(x) M^T \left( I / C + M M^T \right)^{-1} T, \quad (8)$$

where  $C$  is the penalty factor.

Introducing the training error  $\xi_i$  and diagonal matrix  $D$  for weighting, the optimization problem of non-equilibrium learning used to minimize the weighted cumulative error of each sample is expressed as follows:

$$\min \frac{1}{2} \left[ \|\mu\|^2 + C D \sum_{i=1}^N \|\xi_i\|^2 \right], \quad (9)$$

$$\text{s.t. } m(x_i) \mu = t_i^T - \xi_i^T,$$

where  $\mu$  denotes the weight matrix.

The Weighted Gaussian Kernel extreme learning machine is obtained after introducing Gaussian kernel instead of  $M M^T$ ,

$$G(x) = \begin{bmatrix} e^{-\phi \|x-x_1\|^2} \\ \vdots \\ e^{-\phi \|x-x_N\|^2} \end{bmatrix}^T \left[ I / C + D e^{-\phi \|x_i-x_j\|^2} \right]^{-1} D T, \quad (10)$$

where  $\phi$  is the kernel parameter, and  $I$  is the identity matrix.

Obviously,  $C$  and  $\phi$  need to be determined. A Circle chaotic mapping-based GWO is used to determine the parameters,  $C$  and  $\phi$  of WGKELM. In wolf packs, wolves have a strict hierarchical system. When searching for the optimal solution, the grey wolf algorithm selects the best leader wolf  $\alpha$ ,  $\beta$ , and  $\delta$  to lead other grey wolf individuals to hunt within a predetermined search range during each iteration of the search process.

The traditional GWO algorithm is to find the optimal solution during the process of following the leader wolf. However, traditional GWO algorithm restricts the wolves to a single class, forcing the population to converge prematurely and become trapped in local optima. In order to address the limitation of traditional GWO algorithm in the exploration phase where random search cannot traverse the solution space, Circle chaotic mapping is introduced to improve the probability of finding the global optimal solution.

The enhancement procedure that refines the GWO algorithm via Circle chaotic mapping is presented below:

$$x_i(k+1) = \text{mod}\left(x_i(k) + a - \left(\frac{b}{2\pi}\right) \sin(2\pi x_i(k)), 1\right), \quad (11)$$

where  $a, b$  denote the control parameters, and  $\text{mod}()$  denotes the modulo function.

Therefore, Circle chaotic mapping-based GWO algorithm is employed to determine the parameters,  $C$  and  $\phi$  of WGKELM. The processing of determining the parameters,  $C$  and  $\phi$  of WGKELM by using Circle chaotic mapping-based grey wolf optimization algorithm is given as follows:

Step 1. Initialize the range of the parameters,  $C$  and  $\phi$ , and the parameters of GWO are set. The grey wolf population's size is set to 20, randomly generate the grey wolf population, and impose a maximum iteration count of 100.

Step 2. Calculate and rank the fitness values of individual gray wolves, determine their identity, and record relevant location information.

Step 3. Split the grey wolf swarm into  $\alpha, \beta, \delta$  according to the current fitness value.

Step 4. Update the position of each individual according to Eq. (11). Select  $\alpha, \beta, \delta$  from the current wolves based on the fitness value.

Step 5. Prey grey wolves find prey by relying on the information of  $\alpha, \beta, \delta$ .

Step 6. The procedure carries on until the maximum iteration is re-arched, otherwise, loop to Step 2.

#### 4. Experimental Study

In the study, bearing data sets of Case Western Reserve University are used as the experimental data. The state types of the rolling bearings include normal, inner fault, outer fault, ball fault. Here, 200 samples are used as the testing samples, among which there are 50 samples with normal state, 50 samples with inner fault, 50 samples with outer fault, and 50 samples with ball fault. Fig. 2 displays the time-frequency maps of rolling-bearing states generated by empirical wavelet transform, whose texture features are subsequently extracted.

Obtain the training sample set and testing set with low dimensional feature by using ELTSA.  $C$  and  $\phi$  are determined by CGWO. The fault diagnosis model for rolling bearings based on ELTSA and WGKELM with CGWO is obtained. The comparative analysis of the convergence process between CGWO and GWO is given in Fig. 3, and it is obvious that CGWO is better than GWO.

Fig. 4 presents a comparative analysis between the actual results and fault diagnosis results for rolling bearings by using the ELTSA-CGWGKELM method, demonstrating only one misdiagnosed sample. Fig. 5 illustrates the comparison between the actual results and fault diagnosis results for rolling bearings by using the LTSA-WGKELM approach, which exhibits 9 incorrect diagnoses. Similarly, Fig. 6 shows the diagnosis results of LTSA-ELM, with 12 misclassified samples, while Fig. 7 reveals that PCA-ELM yields 16 misclassified samples.

As summarized in Table 1, the fault diagnosis accuracies for rolling bearings are as follows: ELTSA-CGWGKELM achieves 99.5%, LTSA-WGKELM attains 95.5%, LTSA-ELM reaches 94%, and PCA-ELM attains 92%. These results clearly demonstrate that ELTSA-

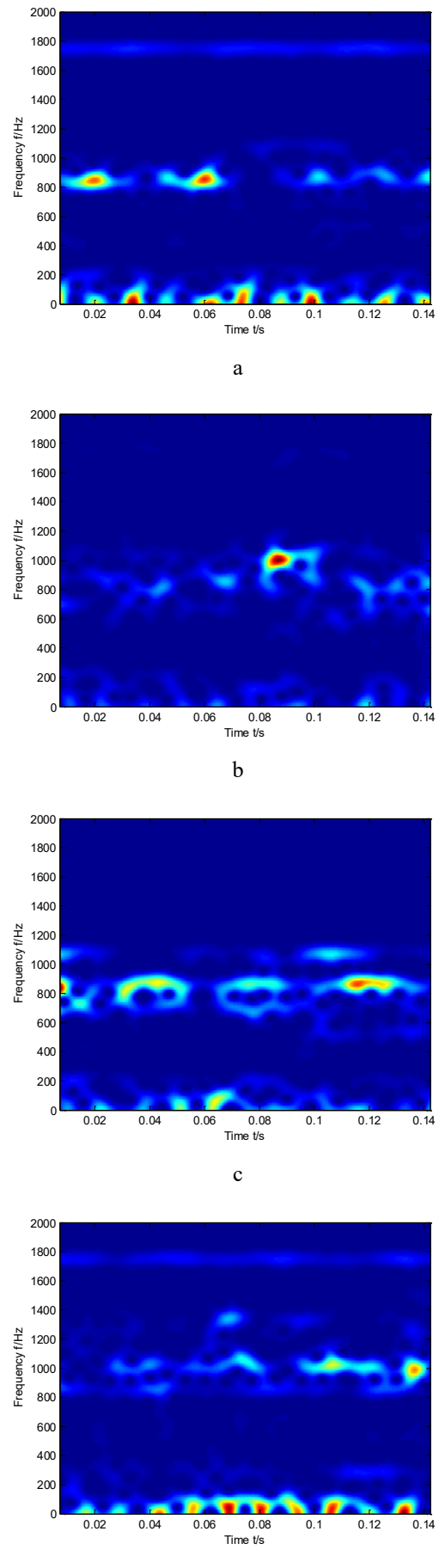


Fig. 2 Time-frequency images of the four state types of a rolling bearing: a – normal state, b – inner fault, c – outer fault, d – ball fault

Table 1  
Comparison of the fault diagnosis results for rolling bearings among ELTSA-CGWGKELM, LTSA-WGKELM, LTSA-ELM, and PCA-ELM

Diagnosis method	The number of the testing samples	The number of the samples with correct diagnosis	Diagnosis accuracy
ELTSA-CGWGKELM	200	199	99.5%
LTSA-WGKELM	200	191	95.5%
LTSA-ELM	200	188	94%
PCA-ELM	200	184	92%

Table 2  
Comparison of the fault diagnosis results for rolling bearings among ELTSA-CGWGKELM, LTSA-WGKELM, LTSA-ELM, and PCA-ELM

Diagnosis method	The number of the testing samples	The number of the samples with correct diagnosis	Diagnosis accuracy
ELTSA-CGWGKELM	150	149	99.33%
LTSA-WGKELM	150	143	95.33%
LTSA-ELM	150	140	93.33%
PCA-ELM	150	137	91.33%

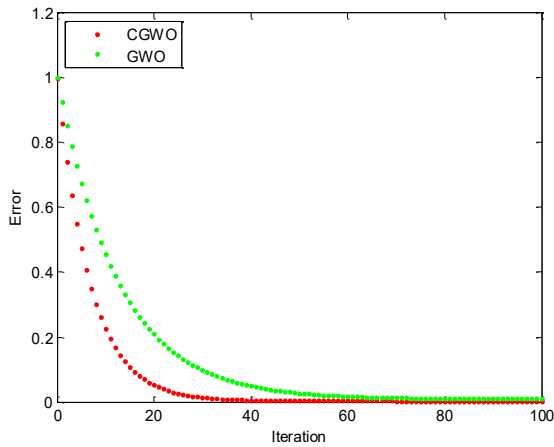


Fig. 3 Comparative analysis of the convergence process between CGWO and GWO

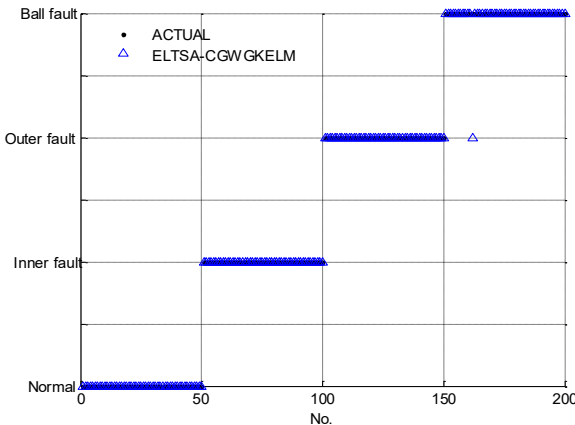


Fig. 4 Fault diagnosis results for rolling bearings of ELTSA-CGWGKELM

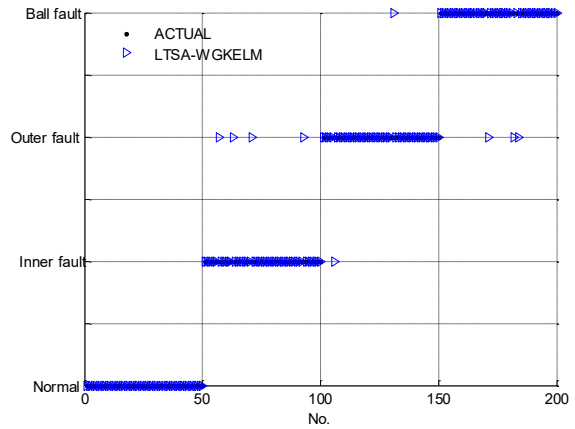


Fig. 5 Fault diagnosis results for rolling bearings of LTSA-WGKELM

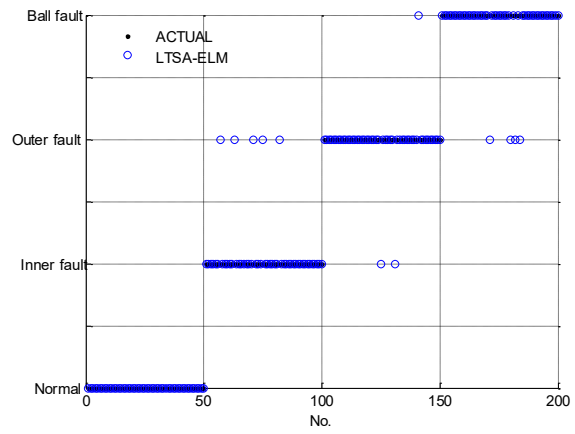


Fig. 6 Fault diagnosis results for rolling bearings of LTSA-ELM

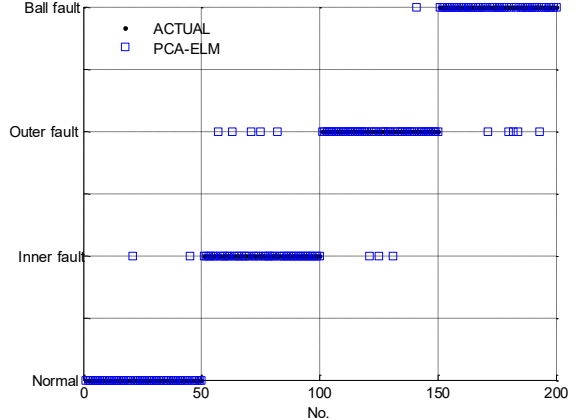


Fig. 7 Fault diagnosis results for rolling bearings of PCA-ELM

CGWGKELM yields higher fault diagnosis accuracy for rolling bearings compared with LTSA-WGKELM, LTSA-ELM, and PCA-ELM.

In order to testify the reliability of the methodology presented in this study, another experimental data from the “Bearing Fault Dataset” provided by Paderborn University are employed.

As summarized in Table 2, the fault diagnosis accuracies for rolling bearings are as follows: ELTSA-CGWGKELM achieves 99.33%, LTSA-WGKELM attains 95.33%, LTSA-ELM reaches 93.33%, and PCA-ELM at-

tains 91.33%. These results clearly demonstrate that ELTSA-CGWGKELM yields higher fault diagnosis accuracy for rolling bearings compared with LTSA-WGKELM, LTSA-ELM, and PCA-ELM.

## 5. Conclusions

This paper presents a fault diagnosis approach for rolling bearings integrating entropy-weighted distance-based Local Tangent Space Alignment (ELTSA) and Weighted Gaussian Kernel Extreme Learning Machine optimized by Circle chaotic mapping-based Grey Wolf Optimization (CGWO). Initially, an innovative ELTSA method is developed to reduce feature dimensionality in rolling bearing data. This enhanced LTSA algorithm addresses limitations in conventional Euclidean distance measurement and improves data information preservation capabilities. Experimental validation confirms that the ELTSA achieves higher sample discrimination rates compared with standard LTSA.

Subsequently, a novel Weighted Gaussian Kernel extreme learning machine (WGKELM) enhanced by CGWO is proposed for rolling bearing fault classification. The WGKELM framework significantly improves nonlinear processing capabilities and robustness over traditional weighted ELM. The CGWO algorithm incorporates circle chaotic mapping to enhance global search efficiency during optimization of WGKELM parameters.

The experimental results indicate the following fault diagnosis accuracy rates for rolling bearings: ELTSA-CGWGKELM achieves 99.5%, LTSA-WGKELM attains 95.5%, LTSA-ELM reaches 94%, and PCA-ELM attains 92% in case 1; ELTSA-CGWGKELM achieves 99.33%, LTSA-WGKELM attains 95.33%, LTSA-ELM reaches 93.33%, and PCA-ELM attains 91.33% in case 2. These results demonstrate that ELTSA-CGWGKELM exhibits superior fault diagnosis capability for rolling bearings compared with LTSA-WGKELM, LTSA-ELM, and PCA-ELM.

## Acknowledgments

This work was supported in part by the Basic Scientific Research Project of Wenzhou under Grant N20240016, and in part by the Science and Technology Research Project of Jiangxi Provincial Department of Education under Grant GJJ212719.

## Conflicts of Interest

We declare that we have no conflicts of interest.

## References

1. Hrcek, S.; Kohar, R.; Brumercik, F.; Kozárik, D.; Steininger, J.; Glowacz, W.; Li, Z. 2025. Proposed methodology for determining the optimal preload of rolling bearings, *Advances in Engineering Software* 209: 104000. <https://doi.org/10.1016/j.advengsoft.2025.104000>.
2. Li, J.; Shi, Q.; Guan, X.; Men, Z. 2025. A similarity-guided block-structured dictionary learning method for fault feature extraction of rolling bearings, *Signal Processing* 238:110195. <https://doi.org/10.1016/j.sigpro.2025.110195>.
3. Gong, F.; Ma, P.; Zhang, H.; Wang, C.; Li, X.; Wu, Y. 2025. Rolling bearings remaining useful life estimation using digital twin and physics-informed methods with uncertainty quantification, *Engineering Applications of Artificial Intelligence* 154: 111070. <https://doi.org/10.1016/j.engappai.2025.111070>.
4. Zhang, K.; Li, B.; Huang, Q.; Gao, S. 2025. A reliability assessment method for rolling bearings under variable speed and variable load conditions, *Measurement* 253: 117571. <https://doi.org/10.1016/j.measurement.2025.117571>.
5. Guo, J.; Wang, M.; Sun, J.; Fang, B.; Chen, F.; Yan, K.; Hon, J. 2025. Behavior of oil droplet swarms during rolling elements-outer ring approach in bearings, *Tribology International* 211: 110910. <https://doi.org/10.1016/j.triboint.2025.110910>.
6. Mishra, C.; Samantaray, A. K.; Chakraborty, G. 2017. Rolling element bearing fault diagnosis under slow speed operation using wavelet de-noising, *Measurement* 103: 77-86. <https://doi.org/10.1016/j.measurement.2017.02.033>.
7. Rohan, A. I.; Ridita, T. A.; Anonto, H. Z.; Hossain, Md. I.; Shufian, A.; Mahin, Md S. R.; Islam, Md, A. 2025. Intelligent fault diagnosis in rolling element bearings: Combining envelope spectrum and spectral kurtosis for enhanced detection, *Results in Engineering* 27: 106899. <https://doi.org/10.1016/j.rineng.2025.106899>.
8. Duda, J.; Leškow, J.; Pawlik, P.; Cioch, W.; 2024. CMAFI – Copula-Based Multifeature Autocorrelation Fault Identification of rolling bearing, *Mechanical Systems and Signal Processing* 211: 111221. <https://doi.org/10.1016/j.ymssp.2024.111221>.
9. Sivalingam, S. M.; Kumar, P.; Govindaraj, V. 2023. A novel numerical scheme for fractional differential equations using extreme learning machine, *Physica A: Statistical Mechanics and its Applications* 622: 128887. <https://doi.org/10.1016/j.physa.2023.128887>.
10. Le, T. T.; Sharma, P.; Bora, B. J.; Kowalski, J.; Osman, S. M.; Le, D. T. N.; Truong, T. H.; Le, H. C.; Paramasivam, P. 2024. Co-gasification of waste biomass-low grade coal mix using downdraft gasifier coupled with dual-fuel engine system: Multi – objective optimization with hybrid approach using RSM and Grey Wolf Optimizer, *Process Safety and Environmental Protection* 191: 234-248. <https://doi.org/10.1016/j.psep.2024.08.066>.
11. Ali, A.; Assam, M.; Khan, F. U.; Ghadi, Y. Y.; Nurdaulet, Z.; Zhibek, A.; Shah, S. Y.; Alahmadi, T. J. 2024. An optimized multilayer perceptron-based network intrusion detection using Gray Wolf Optimization, *Computers and Electrical Engineering* 120: 109838. <https://doi.org/10.1016/j.compeleceng.2024.109838>.
12. Mayet, A. M.; Gorelkina, E. I.; Parayangat, M.; Guarero, J. W. G.; Raja, M. R.; Muqeet, M. A.; Mohammed, S. A. 2024. Enhancing accuracy in X-ray radiation-based multiphase flow meters: Integration of grey wolf optimization and MLP neural networks, *Flow Measurement and Instrumentation* 100: 102734. <https://doi.org/10.1016/j.flowmeasinst.2024.102734>.
13. Singh, K.; Mistry, K. D.; Patel, H. G. 2024. Optimizing power loss in mesh distribution systems: Gaussian Regression Learner Machine learning-based solar irra-

diance prediction and distributed generation enhancement with Mono/Bifacial PV modules using Grey Wolf Optimization, *Renewable Energy* 237: 121590. <https://doi.org/10.1016/j.renene.2024.121590>.

14. **Wang, Z.; Liu, N.; Guo, Y.** 2021. Adaptive sliding window LSTM NN based RUL prediction for lithium-ion batteries integrating LTSA feature reconstruction, *Neurocomputing* 466: 178-189. <https://doi.org/10.1016/j.neucom.2021.09.025>.

15. **Liu, P.; Zhu, X.; Hu, X.; Xiong, A.; Wen, J.; Li, H.; Ai, S.; Wu, R.** 2019. Local tangent space alignment and relevance vector machine as nonlinear methods for estimating sensory quality of tea using NIR spectroscopy, *Vibrational Spectroscopy* 103: 102923. <https://doi.org/10.1016/j.vibspec.2019.05.005>.

Z. Gao, W. Qiu

#### A NOVEL FAULT DIAGNOSIS METHOD FOR ROLLING BEARINGS BASED ON ELTSA AND CGWO-WGKELM

##### Summary

Fault diagnosis method for rolling bearings by using entropy-weighted distance-based local tangent space alignment and Weighted Gaussian Kernel extreme learning machine with Circle chaotic mapping-based grey wolf optimization (ELTSA-CGWGKELM) is presented in this paper. This study introduces two innovative methodologies for rolling bearing fault diagnosis. First, an entropy-weighted distance-based local tangent space alignment

(ELTSA) technique is developed to address feature dimensionality reduction in rolling bearing data. This approach effectively resolves limitations associated with conventional Euclidean distance measurement while significantly enhancing critical data information preservation capabilities. Secondly, a weighted Gaussian kernel extreme learning machine optimized through circle chaotic mapping-enhanced grey wolf optimization (CGWGKELM) is proposed for fault classification. The Gaussian kernel implementation substantially improves nonlinear processing performance and robustness compared with traditional weighted ELM architectures. The circle chaotic mapping strategy integrated into the grey wolf optimization algorithm (CGWO) enables superior optimization of the weighted Gaussian kernel ELM training parameters, ensuring enhanced global search capability and convergence efficiency. The experimental results indicate the following fault diagnosis accuracy rates for rolling bearings: ELTSA-CGWGKELM achieves 99.5%, LTSA-WGKELM attains 95.5%, LTSA-ELM reaches 94 %, and PCA-ELM attains 92% in case 1; ELTSA-CGWGKELM achieves 99.33%, LTSA-WGKELM attains 95.33%, LTSA-ELM reaches 93.33%, and PCA-ELM attains 91.33% in case 2. It is indicated that ELTSA-CGWGKELM is the better fault diagnosis ability for rolling bearings than LTSA-WGKELM, LTSA-WGKELM, and PCA-ELM.

**Keywords:** ELTSA, CGWGKELM, circle chaotic mapping, intelligent diagnosis.

Received August 27, 2025

Accepted December 15, 2025



This article is an Open Access article distributed under the terms and conditions of the Creative Commons Attribution 4.0 (CC BY 4.0) License (<http://creativecommons.org/licenses/by/4.0/>).